Electronic Supplementary Material (ESI) for Journal of Materials Chemistry A.

Supporting Information

Experimental and Computational Studies of Formic Acid Dehydrogenation over PdAu: Influence of Ensemble and Ligand Effects on Catalysis

Jin Hee Lee, Jinwon Cho, Mina Jeon, Muhhamad Ridwan, Hyun Seo Park, Sun Hee Choi, Suk Woo Nam, Jonghee Han, Tae-Hoon Lim, Hyung Chul Ham,* Chang Won Yoon*

Table S1. The calculated total energy changes (ΔE) and activation barriers (Ea in parenthesis) for dehydrogenation steps with the pure Pd and PdAu catalysts. The units are given in eV.

ΔE (Ea)/ eV	Pd_4/Au_4 $/Pd_2Au_2(111)$ (**I**)	Pd_3Au_1/ Pd_1Au_3 $/Pd_2Au_2(111)$ (**II**)	Pd_2Au_2/ Pd_2Au_2 $/Pd_2Au_2(111)$ (**III**)	$Pd_1Au_3/ Pd_3Au_1/$ Pd_2Au_2 (111) (**IV**)
[D1] HCOOH → HCOO + H	-0.14/(0.79)	-0.18/(0.60)	0.07/(0.87)	0.81/(1.40)
[D2] HCOO → CO_2 + H	-0.41/(0.92)	-0.70/(0.87)	-0.43/(1.13)	-0.67(0.89)

Table S2. Pd 3d XPS peak positions and relative peak areas of the catalyst **1**-**3.**

$PdAuAl_2O_3$-CO (**1**)		$PdAuAl_2O_3$-H_2 (**2**)		$PdAuAl_2O_3$-N_2 (**3**)	
Peaks/ eV	Area/ %	Peaks/ eV	Area/ %	Peaks/ eV	Area/ %
335.41	39	335.45	34	335.42	37
336.93	21	336.76	26	336.71	23
340.67	26	340.71	23	340.68	25
342.19	14	342.02	17	341.97	15

Table S3. Relative ratios of CO adsorbed on Pd hollow and atop sites.

Catalysts	Hollow/ %	Bridge/ %	Atop/ %
$PdAuAl_2O_3$-CO (**1**)	34	54	12
$PdAuAl_2O_3$-H_2 (**2**)	23	60	17
$PdAuAl_2O_3$-N_2 (**3**)	8	70	22
Pd/Al_2O_3 (**4**)	22	67	11

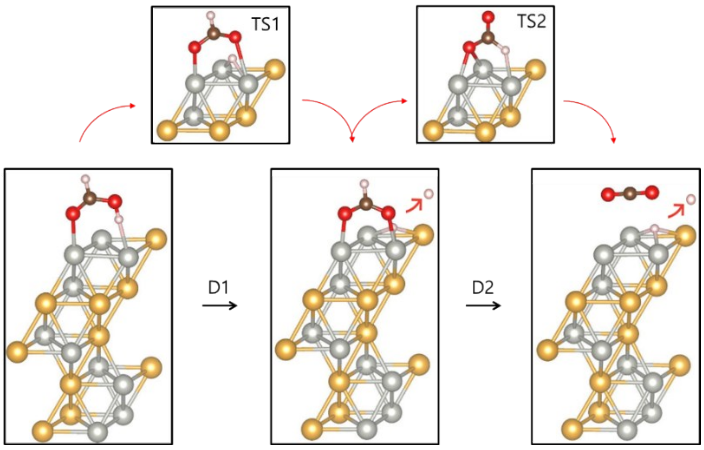

Fig. S1. Calculated dehydrogenation steps for $Pd_3Au_1/Pd_1Au_3/Pd_2Au_2(111)$ (**II**). Direct pathway to HCOO+H then to COO+2H is indicated as D1 and D2. The TS1 and TS2 indicate the structure of transition states of step D1 and D2, respectively. The gray, yellow, brown, red and white balls represent Pd, Au, C, O, and H atoms, respectively.

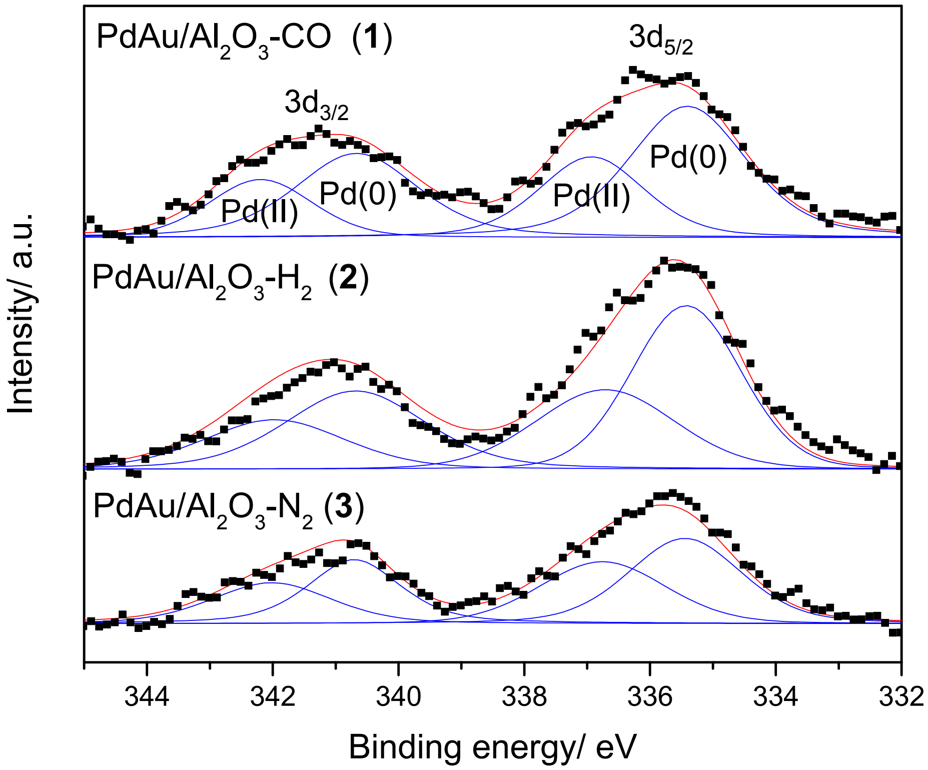

Fig. S2. The Pd 3d XPS spectra of the as-prepared catalysts, **1**-**3**.

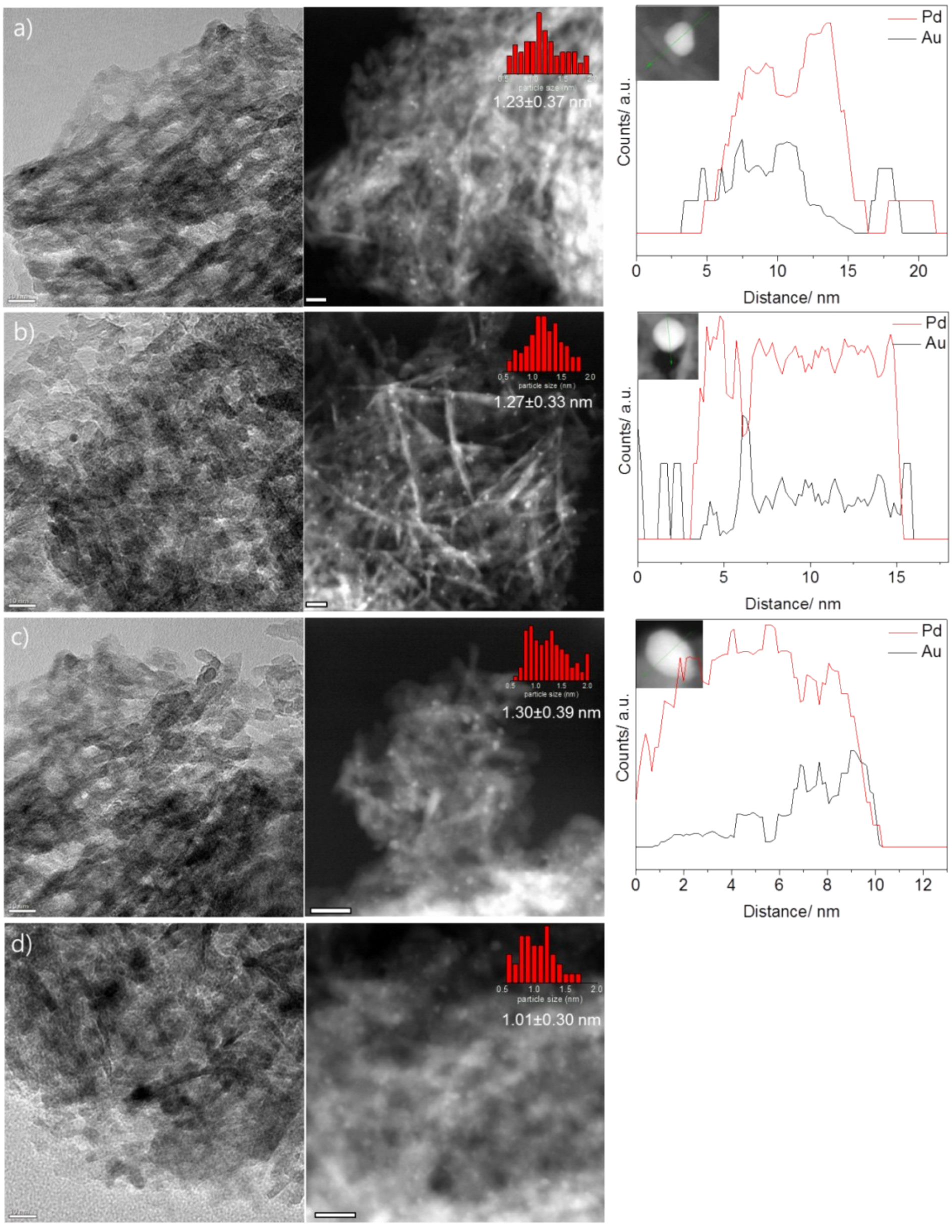

Fig. S3. TEM and STEM images of the as-prepared catalysts, their particle size distributions (inset) and EDS line profiles: a) PdAu/Al_2O_3-CO (**1**), b) PdAu/Al_2O_3-H_2 (**2**), c) PdAu/Al_2O_3-N_2 (**3**), and d) Pd/Al_2O_3 (**4**). Scale bars are 10 nm in size.

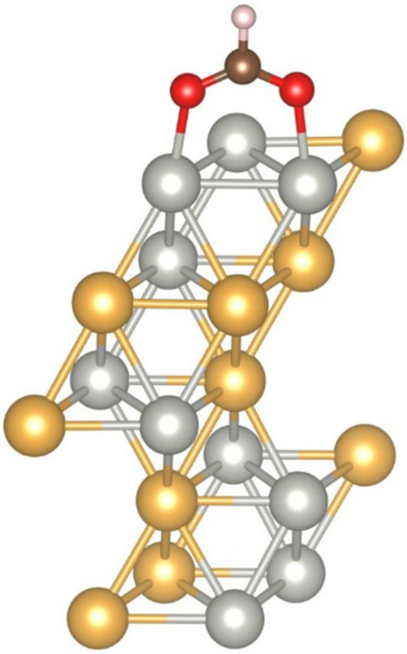

Fig. S4. Optimized structure of HCOO absorbed on the top site of $Pd_3Au_1/Pd_1Au_3/Pd_2Au_2$ (**II**).

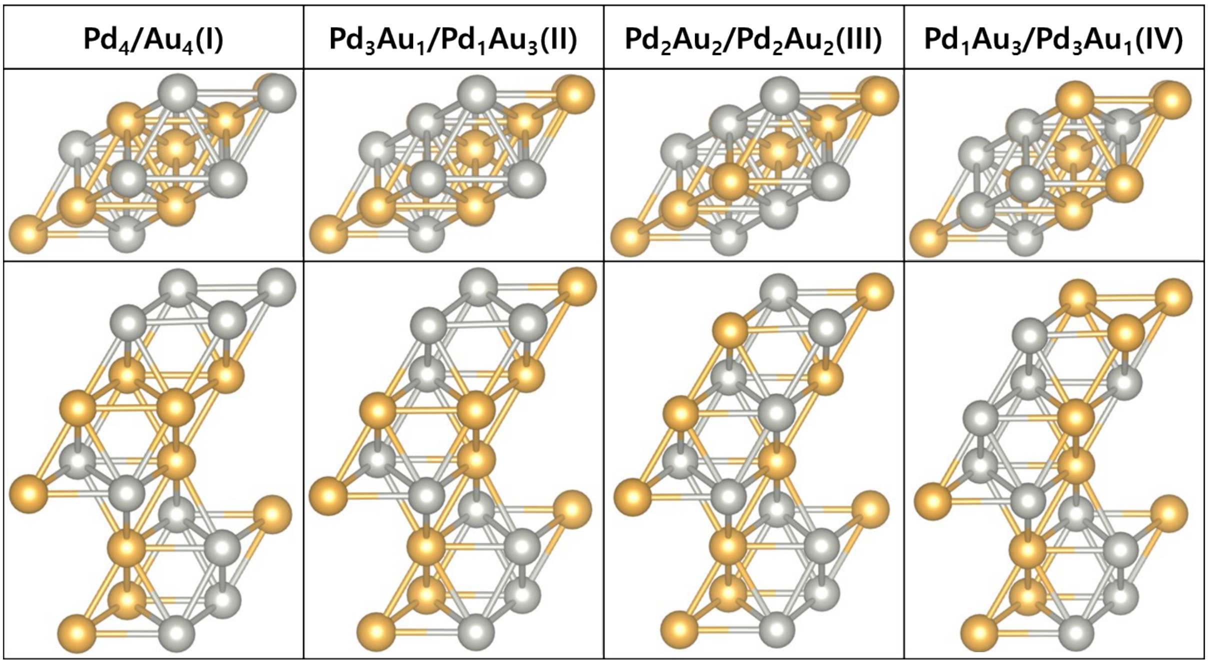

Fig. S5. The surface models used in this study in top view (top) and side view (bottom). The grey and gold balls represent Pd and Au atoms respectively.

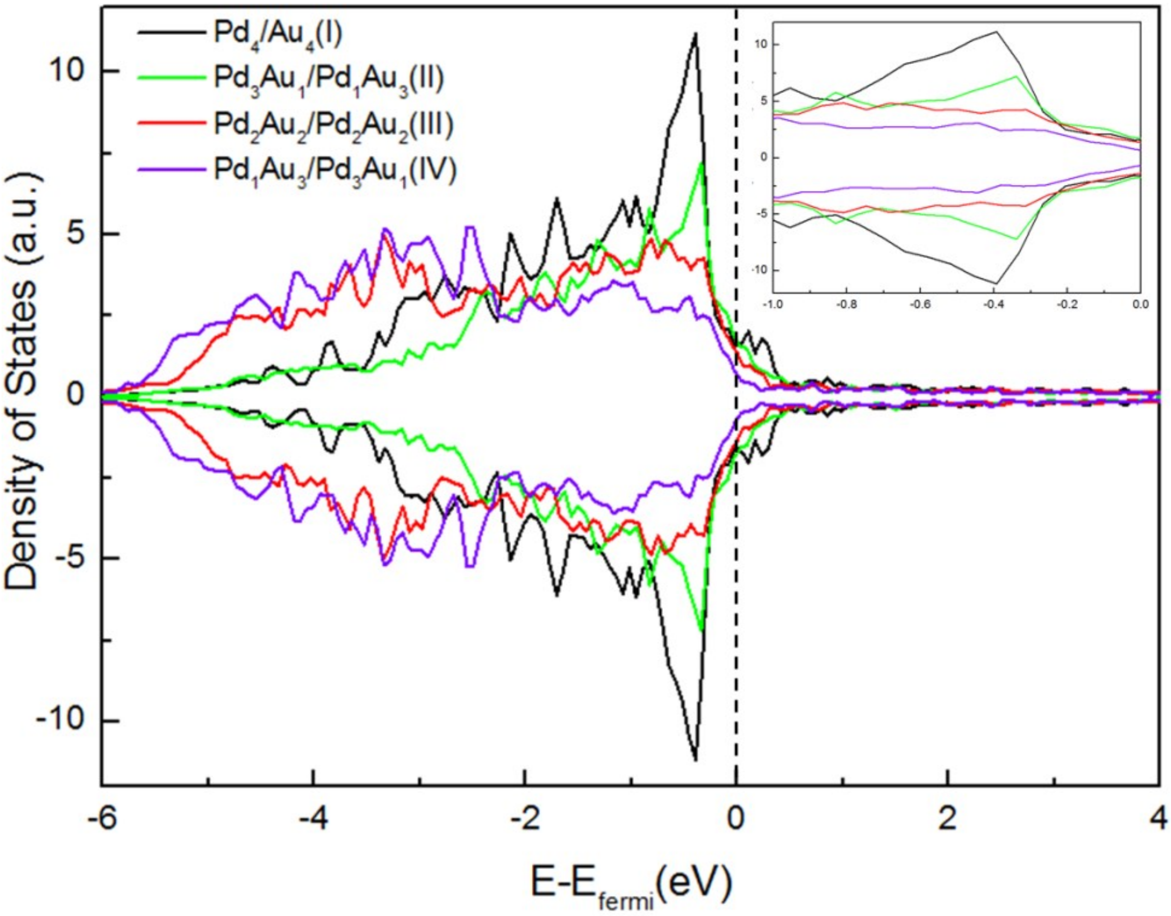

Fig. S6. Projected local density of states (LDOS) plots on the d states of the surface for the I, II, III, and IV. The displayed vertical line at 0 eV stands for the Fermi level.

As a number of Pd atoms in the surface decreases, density, in a range between -2eV and 0eV, also down shifts due to the charge transfer from the surface Au atom to the subsurface Pd atoms and thus the total number of charge on the surface decreases as well. The upper right-hand graph shows the enlarged LDOS in a range of -1eV to 0eV. Among the surface models, II (shown in green) has the highest density near the fermi level which suggests higher the activity of surface atoms toward chemisorption and as in Table 1 the CO binding energy of II is ΔE = -0.05eV energetically more favourable than I, III and IV.

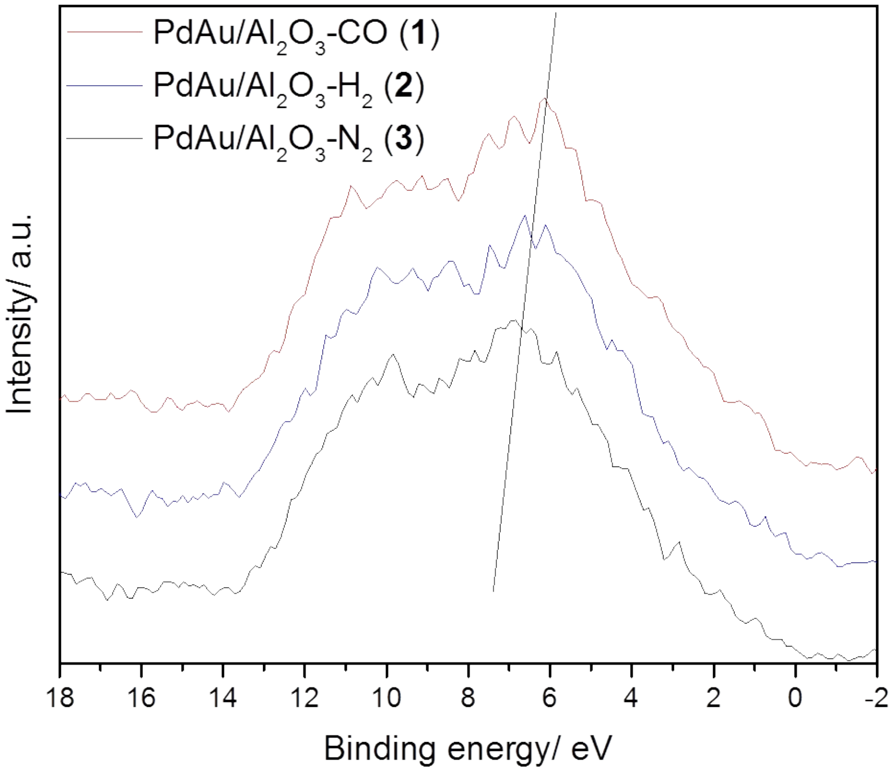

Fig. S7. Valance XPS spectra of the catalysts **1**-**3**.

The down shift of the peak near the Fermi level was observed by valance XPS measurement and it successfully proved the *d*-band structure of model catalysts obtained by DFT calculation.